actuators

MDPI

Article

Self-Healing and High Interfacial Strength in Multi-Material Soft Pneumatic Robots via Reversible Diels–Alder Bonds

Seppe Terryn [1,2,*], Ellen Roels [1,2], Joost Brancart [2], Guy Van Assche [2] and Bram Vanderborght [1]

1 Brubotics, Vrije Universiteit Brussel (VUB) and Flanders Make, Pleinlaan 2, B-1050 Brussels, Belgium; ellen.roels@vub.be (E.R.); bram.vanderborght@vub.be (B.V.)

2 Physical Chemistry and Polymer Science (FYSC), VUB, Pleinlaan 2, B-1050 Brussels, Belgium; joost.brancart@vub.be (J.B.); Guy.Van.Assche@vub.be (G.V.A.)

* Correspondence: seterryn@vub.ac.be; Tel.: +32-499-26-74-73

Received: 3 April 2020; Accepted: 28 April 2020; Published: 30 April 2020

Abstract: In new-generation soft robots, the actuation performance can be increased by using multiple materials in the actuator designs. However, the lifetime of these actuators is often limited due to failure that occurs at the weak multi-material interfaces that rely almost entirely on physical interactions and where stress concentration appears during actuation. This paper proposes to develop soft pneumatic actuators out of multiple Diels–Alder polymers that can generate strong covalent bonds at the multi-material interface by means of a heat–cool cycle. Through tensile testing it is proven that high interfacial strength can be obtained between two merged Diels–Alder polymers. This merging principle is exploited in the manufacturing of multi-material bending soft pneumatic actuators in which interfaces are no longer the weakest links. The applicability of the actuators is illustrated by their operation in a soft hand and a soft gripper demonstrator. In addition, the use of Diels–Alder polymers incorporates healability in bending actuators. It is experimentally illustrated that full recovery of severe damage can be obtained by subjecting the multi-material actuators to a healing cycle.

Keywords: self-healing polymers; biomimetic; bioinspired robotics; soft robots; soft grippers

1. Introduction

Soft robots arose from the need for robots that interact safely with unknown environments and that can assist people in close contact [1]. This new generation of robots is partially or completely constructed out of flexible materials, such as silicones or polyurethanes [2,3]. Because of their intrinsic compliance, they can safely interact with their surroundings. Many are pneumatically driven [4–6], exploiting the compressibility of gas, incorporating compliance that provides both safety [7,8] and energy efficiency [9]. Because of their intrinsic compliance and safety, these soft robots will be deployed in applications where delicate tasks have to be performed, including minimal invasive surgery [10], active prosthetics [11] and automation tasks that involve manipulating delicate objects with irregular shapes. The latter tasks will be performed by soft grippers [12,13], constructed out of flexible membranes that allow them to gently pick and place delicate soft objects, such as fruit and vegetables in agricultural applications or in food packaging industries [14].

Soft robots that consist almost entirely out of a single highly flexible materials, are referred to as continuum soft robots [1,2,15] and have very limited force output. However, medium to high force outputs are often required for grasping, picking, and manipulation. Using multiple materials in a single design can improve the actuator's performance [16,17]. The use of multiple flexible materials with

different mechanical properties can allow creating (anisotropic) deformation responses that cannot be obtained in single-material actuators, as well as more complex embodied intelligent behaviors [18–20]. Combining less flexible or even stiff materials with flexible membranes in articulated soft robots [21,22] allows greatly increasing the force output. However, in multi-material soft robotic components the connections between different flexible materials and the connections between flexible and non-flexible materials are generally weak. This is because they rely fully on physical adhesion. Over time or when extensively loaded, the components fail at these interfaces, where stress concentrations build up during actuation. In multi-material soft pneumatic actuators, leaks will occur at the material interfaces, leading to a decrease in actuation efficiency and performance, and eventually to failure of the component at a limited lifetime.

In this paper, we propose to solve this problem by constructing novel multi-material soft pneumatic actuators out of multiple Diels–Alder (DA) polymers [23–26]. These are elastomeric polymer networks of which the crosslinks are reversible DA bonds. DA polymers can be synthesized with very distinctive characteristics, e.g., mechanical properties at room temperature, by changing the monomer units and/or the ratio between them [27,28]. As all produced networks contain the same DA crosslinks, covalent bonds can be formed across the contact interface between DA polymers with completely different mechanical properties, by means of a mild heating procedure. The interfacial strength of the merged region between two different DA polymers will be experimentally validated in this paper.

This merging principle can be exploited in the manufacturing of multi-material soft robots, as will be demonstrated by the development of a self-healing bending soft pneumatic actuator, made from two DA materials. The manufacturing of this actuator relies on a shaping technique that exploits the merging principle and is noted as the "folding and covalently binding" technique. In previous research this technique was used to manufacture single-material self-healing soft actuators [27]. This paper reports on the use of this manufacturing technique with multiple DA polymers. Five of these multi-material actuators were produced and their mechanical properties as well as their robustness are validated and will presented. The usability of the newly developed actuators will be demonstrated by using four to form a soft gripper designed to handle delicate objects and five as the fingers of a soft hand, suitable for social robotics applications.

Using DA polymers to construct soft robot components has an additional advantage, it integrates a healing ability that allows recovering completely from macroscopic damages, as already demonstrated in previous work [27–29]. In this paper, it will be illustrated that in the developed actuator prototype large cuts and perforations can be completely healed as well, by use of a heat–cool cycle using moderated temperatures. Finally, the recovery of the actuator properties after healing will be investigated.

2. Materials and Methods

2.1. Reagents

Furfuryl glycidyl ether (FGE, 96%) was obtained from Sage Chemicals. 1,1′-(methylenedi-1,4-phenylene)bismaleimide (DPBM, 95%) was obtained from Sigma Aldrich. Jeffamine JT5000 (poly(propylene glycol) bis(2-aminopropyl ether)) with average molecular weight of 5649 g.mol^{-1} (NMR) was obtained from Aurora Chemicals The reagents and their schematic representation are listed in Figure 1.

2.2. Synthesis

The synthesis of DA polymer networks is performed in two steps. First, the FGE is irreversibly bonded to the Jeffamine (JT5000) by way of an epoxy-amine reaction to yield a furan-functionalized Jeffamine (FT5000). FGE and JT5000 are mixed in stoichiometric epoxy-amine ratio and left for 5 days at 60 °C and another 2 days at 90 °C, to complete the irreversible reaction between these two components. Next furan groups on the furan-functionalized Jeffamine are reacted with the maleimide groups on a bismaleimide to form DA crosslinks that form a thermoreversible network (DPBM-FT5000), through

solvent casting. DPBM and FT5000 are dissolved in chloroform ($CHCl_3$) (20 wt.%). The network is formed by extracting the chloroform in vacuum at 110 °C for 2 h after which the material is cooled down to 25 °C (0.5 K min^{-1}). More details on the synthesis can be found in the supplementary materials of [27].

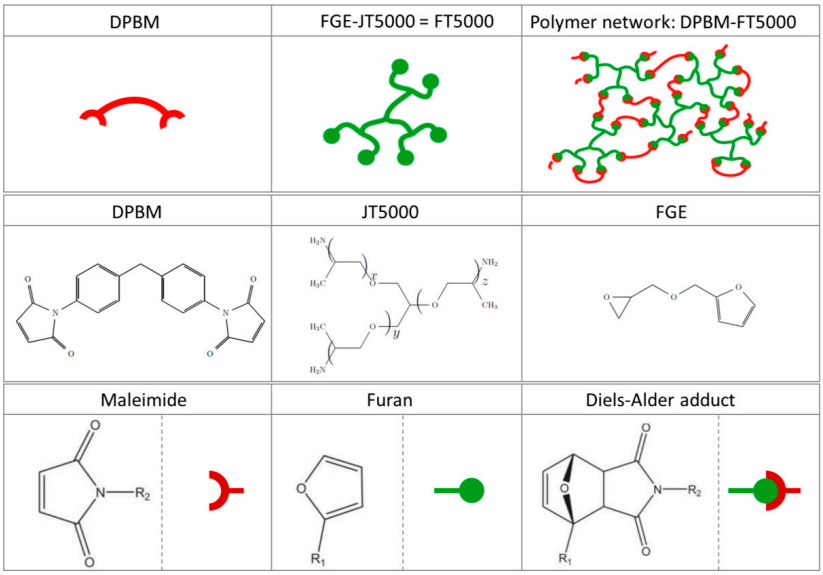

Figure 1. Reagents used in to synthesize the Diels–Alder polymer networks and their schematic representation.

2.3. Diels–Alder Network Characteristics

The material properties of the Diels–Alder networks can be changed, according to the demands of the applications in which these materials are used, by changing network design parameters. These parameters are the molar mass of the reagents, the functionality of the reagents and the ratio between the reactive components, in this case maleimide and furan. In this paper, two Diels–Alder networks, DPBM-FT5000-r = 1 and DPBM-FT5000-r = 4/6 are used (Figure 2). These differ in maleimide-to-furan ratio (r). The characteristics of the networks are derived in previous work [28] and listed in Table 1. For the DPBM-FT5000-r = 1 a stoichiometric maleimide-to-furan ratio was used during the synthesis. In the synthesis of the DPBM-FT5000-r = 4/6 network a deficit of maleimide was used, resulting in r = $[M_0]/[F_0]$ = 4/6. Changing the r-ratio, leads to a change in crosslink density and this directly affects the mechanical properties of the network. A deficit in reactive maleimide decreases the crosslink density, which leads to an increase in flexibility, visible by a decrease in Young's modulus E (Table 1). The r-ratio also affects the gel transition temperature, the temperature at which the polymer transforms from a solid network structure to a viscous liquid (upon heating). Networks with a lower r-ratio degel into a viscous liquid state at a lower temperature and can therefore be reshaped and reprocessed at lower temperatures. Both networks used in this paper, DPBM-FT5000-r = 1 and r = 4/6 are hyper flexible materials (Table 1), as illustrated by the low Young's moduli (E) and the high fracture strains (σ_{max}). This makes them suitable for soft robotics applications.

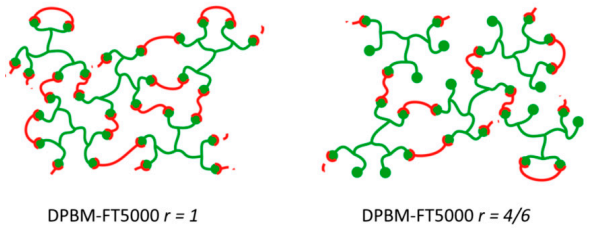

Figure 2. By changing the maleimide-to-furan ratio (r) the crosslink density can be varied. This results in a change in material properties of the synthesized networks.

Table 1. Characteristics of the JT5000-based networks, derived in previous work [28].

DA network	*r*	$[F_0]$ (mol kg^{-1})	$[M_0]$ (mol kg^{-1})	T_{gel} (°C)	T_g (°C)	E (MPa)	σ_{max} (MPa)	ε_{max} (%)
DPBM-FT5000-*r1*	1	0.77	0.77	110	−64.3	8.21	1.20	150
DPBM-FT5000-*r4/6*	4/6	0.81	0.54	102	−64.2	0.72	0.40	144

2.4. Healing in Diels–Alder Networks

The reversible crosslinks in DA networks allow healing macroscopic damages (Figure 3). When damaged, at the location of the fracture, DA bonds will break, because these are the weakest covalent bonds in the networks. DA networks are non-autonomous self-healing polymers, meaning their healing procedure requires a stimulus in the form of heat. The healing procedure has a total duration of 24 h and the temperature-time profile is represented in Figure 4. To initiate, the network is heated to a few tens degrees below the (de)gelation temperature (T_{gel}). This temperature (T_{max} = 80 – 90 °C) cannot exceed the T_{gel}, because this leads to a loss of structural stability. At this temperature, the crosslink density will decrease, because the equilibrium shifts towards the formation of reactive maleimide and furan by breaking a portion of the DA bonds. The decrease in crosslink density results in an increase in molecular mobility. This increased mobility allows gradual sealing of the fracture. This takes time (order of minutes), which is why the polymer must remain at this temperature for 20-60 min (t_{iso} in Figure 4), depending on the size of the damage. When the fracture is completely sealed, the network is cooled down. During cooling the equilibrium shifts back towards the formation of DA bonds and the crosslink density increases. Throughout the material as well as across the fracture area DA crosslinks are formed. At room temperatures, the kinetics of the DA reaction are relatively slow. Consequently, the formation of DA bonds requires time and as such the network is kept at room temperature for 24 h. After 24 h, a near equilibrium DA crosslink density is achieved and the material is as good as new. No weak spots are created at the location of the "scar", as result of the strong DA bonds formed across the fracture area. Because the network recovers completely its initial properties, healing in DA polymers can be performed multiple times.

2.5. Merging of Diels–Alder Parts, Possibly with Different Properties

By varying the network design parameters, DA networks can be synthesized with material properties that vary over a broad range. However, all these networks contain the same reversible crosslinks, the DA bonds. As such, two DA parts with different material properties (Figure 5) can be merged by bringing the parts in contact on a microscopic level and performing a heat–cool cycles with a temperature-time profile similar to the one presented in Figure 4. The result of this merging process is a strong interface between the two DA materials, due to the covalent DA bonds formed across the interface. This merging principle can be used in the manufacturing of multi-material soft robots and can increase the robustness of these systems, in which damages usually occur after a high number of actuation cycles at the multi-material interfaces, where stress concentration points are formed during actuation.

2.6. Manufacturing Through Folding and Covalently Binding

The merging principle of DA networks can be exploited in the manufacturing of multi-material self-healing soft robotics. The DA networks are synthesized through solvent casting, during which sheets are formed. In search of manufacturing methods to reshape these sheets into three-dimensional soft robotics components, a new shaping technique was developed; "Folding and Covalently Binding (FCB)", described in detail in [27]. Using this principle, 3D hollow polygon objects can be created by subsequently folding sheets and binding edges together (Figure 6). When folding a sheet into a 3D structure inside a mold at room temperature, the elastic behavior that is predominant over the viscous behavior in this visco-elastic network, generates stresses at the creases (Figure 6B). These stresses

induce an elastic response when the part is removed from the mold, which unfolds the part back into a sheet. However, the stresses within the folded part inside the mold can be relaxed by increasing the viscous portion in visco-elastic behavior through heating (Figure 6C). When all stresses are relieved, the part can be cooled down and demolded. Due to the stress relaxation it remains in the folded state at room temperature (Figure 6D). 3D DA parts can be joined to other DA parts, with possibly different mechanical properties, through the merging principle using a heat–cool cycle (Figure 6E). The result is a 3D part that is form stable at moderate temperatures and in which the merged regions have a high interfacial strength (Figure 6F). This shaping method will be illustrated in Section 3.3 by the manufacturing of a multi-material soft pneumatic actuator.

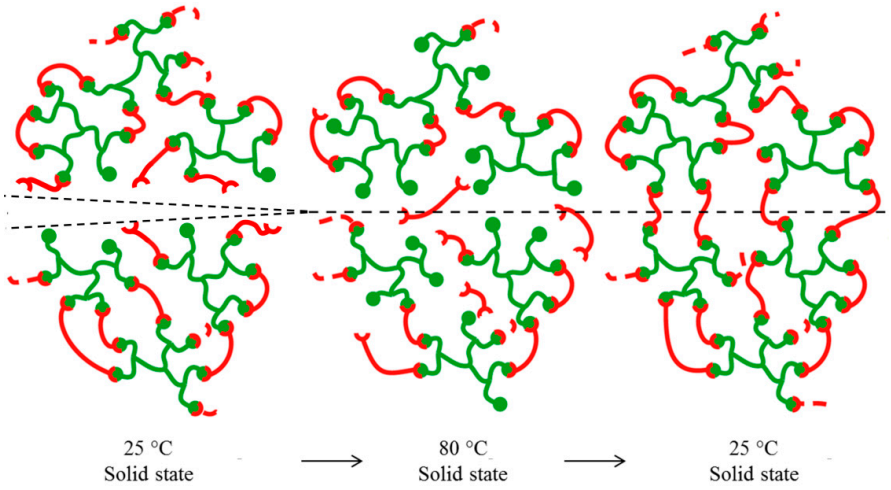

Figure 3. Damage in a DA part can be healed using a mild heating treatment. The result is a strong interface due to covalent DA bonds at the location of the scar and full recovery of the initial properties.

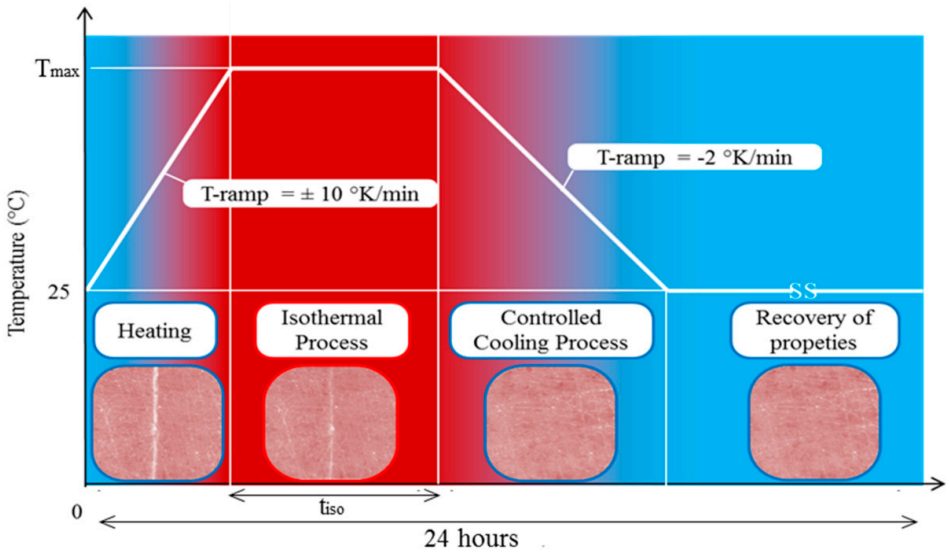

Figure 4. Temperature profile of the healing procedure for a macroscopic damage. The pictures illustrate the healing of a cut (length = 10 mm and width = 0.1 mm) in a DPBM-FT5000-r4/6 sheet, with a thickness of 0.75 mm. This damage is completely healed after healing (adapted from [27]).

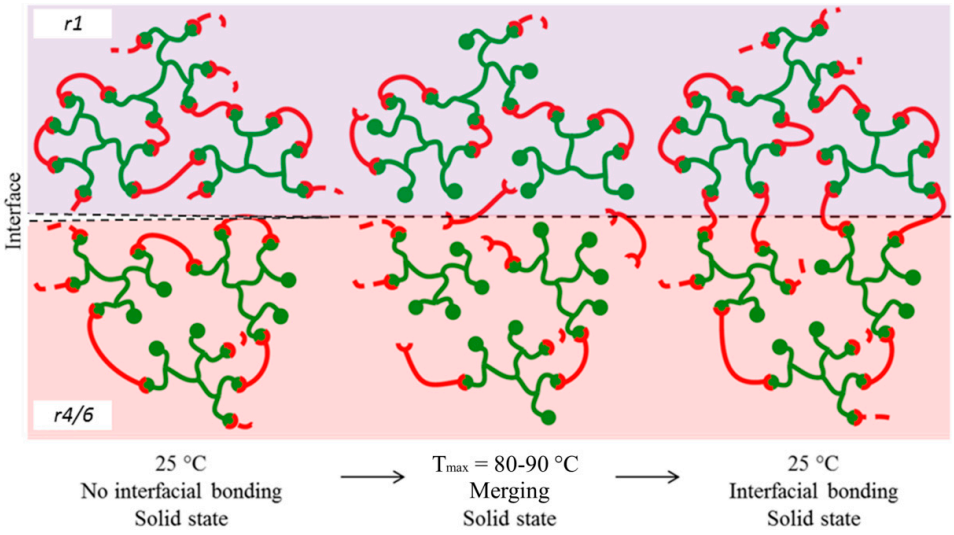

Figure 5. Separated DA parts (possibly with other material properties) can be merged using a mild heating treatment. The result is a strong interface due to covalent DA bonds.

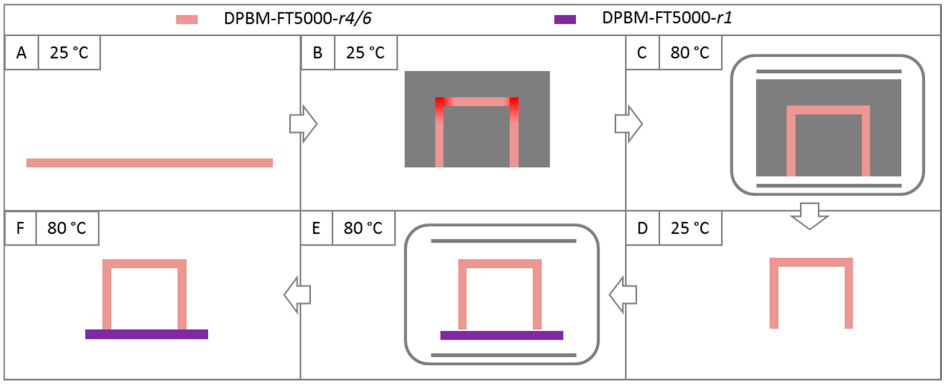

Figure 6. Schematic on the novel manufacturing technique based on Folding and Covalently Binding (FCB) using multiple DA networks. (**A**) DA parts are synthesized into sheets. (**B**) DA sheets are folded and kept from unfolding by placing it a mold. At the creases, the folding induces stresses. (**C**) The induced stresses can be relaxed by increasing the temperature. (**D**) When cooling down, the part remains form stable in its folded state. (**E**) DA parts, with possibly different mechanical properties can be joined using a heat–cool cycle with a temperature profile as presented in Figure 4. (**F**) The result is a 3D polygon (multi-material) structure with structure stability up to moderated temperatures (< T_{gel}) and in which the merged regions have a high interfacial strength.

3. Results

3.1. Validation of the Merging Principle

To illustrate that high interfacial strength can result from merging two different DA networks, merged tensile samples (length: 7.79 ± 0.37, width: 5.54 ± 0.02 and thickness: 2.19 ± 0.08) were created that consist partly out of DPBM-FT5000-r1 (referred to as r1) and partly out of DPBM-FT5000-r4/6 (r4/6) (Figure 7B). The merged samples were created by bringing the two materials in contact and subjecting them to a heat–cool cycles with varying maximum temperatures (T_{max}) of 75 °C, 80 °C, 85 °C and 90 °C with a duration of the isothermal (t_{iso}) of 1 h (Figure 4). For each of the merging temperatures, 6 tensile samples were manufactured and tested in a tensile test until fracture with a strain rate of 1 %min^{-1} at 25 °C. As a reference, 6 single-material tensile samples, made from the least crosslinked and weakest DA material, r4/6, were tested as well (Figure 7A). These single-material

samples fractured with a clean fracture surface, without the occurrence of necking at stresses of 0.40 ± 0.01 MPa. From the fracture stress data of the multi-material tensile samples in Figure 7E, it is clear that for an increased healing temperature, the fracture stress increases. To ensure a firm, covalently bound interface, two criteria must be met during the heat–cool cycle: a good contact is required at the microscopic level, and sufficient DA bonds must be broken and reformed. If heated to 70 °C, which is 32 °C below T_{gel} of r4/6 (Table 1), the fracture takes place at low stress values and at the interface (Figure 7C). Using low healing temperatures relatively to T_{gel}, such as at 70 °C, a low fraction of DA bonds will be broken. As a result, only a few DA bonds can be formed across the interface upon cooling, resulting in a weaker interfacial strength at 25 °C. When the temperature of the heating stage is increased to 75 °C and 80 °C, the interfacial strength increases (Figure 7E), because more DA bonds can be formed across the interface between r1 and r4/6. Additionally, when more DA bonds are broken, the microscopic mobility in the polymers increases, which improves the microscopic contact, enhancing interfacial bonding even further.

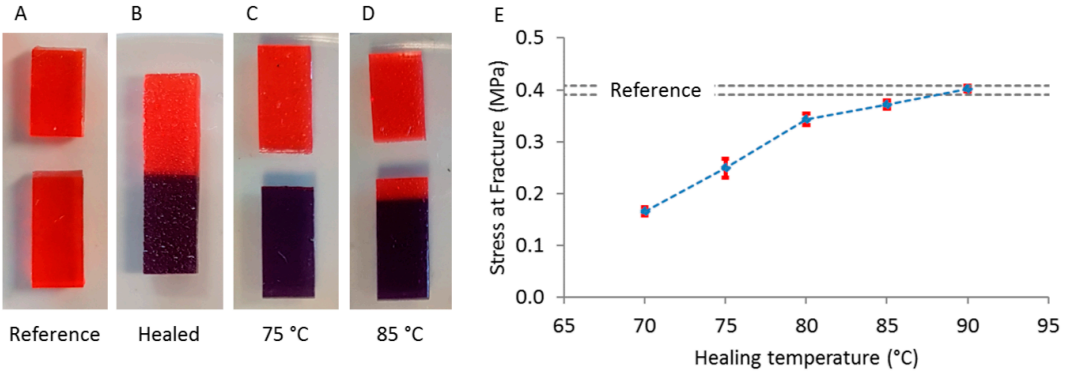

Figure 7. (**A**) A single-material r4/6 tensile sample used as a reference. (**B**) r1 (purple)–r4/6 (red) samples, merged by a heat–cool cycle with a maximum temperature of 70 °C, 75 °C, 80 °C, 85 °C or 90 °C. (**C**) Tensile samples that are merged at 70–80 °C fracture at the multi-material interface. (**D**) Tensile samples that are merged at 85–90 °C do not fracture at the multi-material interface. (**E**) The measured fracture stresses as function of the merging temperature. These were measured in a tensile test until fracture with a strain ramp of $1\%s^{-1}$ at 25 °C on samples with a length 7.79 ± 0.37, a width of 5.54 ± 0.02 and thicknesses of 2.19 ± 0.08. Mean values and standard errors of the mean (SEM) are presented.

When heated to 85 °C or higher, the fracture does not take place at the interface, but in the weakest material (r4/6: red in Figure 7D). The interface can withstand higher stresses than r4/6, and the sample fails in the r4/6 region at similar fracture stresses as those found for the single-material reference samples. From this, we can conclude that when the two DA polymers are joined and heated to a few degrees below the lowest T_{gel}, the interfacial bond is stronger than the strength in the bulk of the pure material with the weakest mechanical properties. This merging procedure is limited by T_{gel}, because at higher temperatures the less crosslinked material will lose its structural integrity and starts flowing.

3.2. Design of the Prototype

To validate both the merging principle and the healability, a multi-material self-healing soft pneumatic actuator (Figure 8) is developed based on PneuNets designs [3,11,30]. Soft pneumatic actuators are usually constructed out of elastomeric polymers that in most cases have a nearly isotropic strain response to stresses, as in the case of silicones and polyurethane. Bending motions in single-material actuators can be created through design, as illustrated in [3,11,27,30]. However, in many cases, the anisotropic deformations of soft actuators are enhanced by using less flexible materials in the design, restricting strains in a certain direction [31]. The produced bending soft pneumatic actuator (BSPA) consists of nine air chambers constructed from the highly flexible r4/6-network. The bottom layer is made from the less flexible r1-network. The higher modulus of the bottom layer limits planar

strains and enhances the bending deformation upon pressurizing the air chambers. These air chambers are interconnected through open spaces between the bottom layer and the top part containing the air chambers. Because of the merging principle between both DA networks, r1 and r4/6, this actuator will be robust.

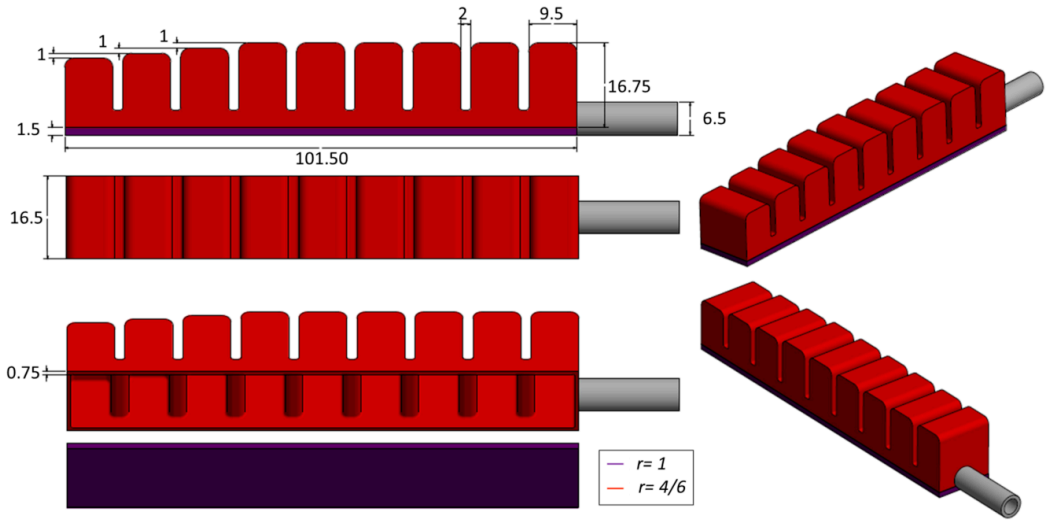

Figure 8. Design of the multi-material self-healing bending soft pneumatic actuator: The air chambers are made using a soft DA network, DPBM-FT5000-r4/6, while the bottom layer is made from a less flexible DA network, DPBM-FT5000-r1. As a result, the anisotropic deformation response of the actuator to an applied stress induced by pressurizing the air chambers is enhanced. Dimensions are presented in millimeters.

3.3. Manufacturing

The manufacturing of this multi-material BSPA relies on the folding and covalently binding technique (Section 2.6). This technique can be used to construct multi-material 3D polygon structures from DA sheets, as is illustrated by the steps required to produce multi-material BSPAs in Figure 9.

Figure 9. Manufacturing process of the multi-material self-healing bending soft pneumatic actuator constructed out of DPBM-FT5000-r4/6 (red) and r1 (purple).

A. r4/6 and r1 are synthesized by solvent-casting thin sheets with dimensions: $100 \times 100 \times 0.75$ mm^3.
B. A 3D printed, polylactic acid (PLA) mold is used to fold a r4/6 sheet. The mold consists of several different parts: a large bottom part containing the square wave shape of the top layer of the actuator, and nine smaller individual molds with the shape of the air chambers.
C. First thin strips of $100 \times 16.5 \times 0.75$ mm^3 of r4/6 are cut from the synthesized sheets. The ends of four of these strips are merged, using a local heating procedure of 120 °C using a soldering tool, to form a strip of $400 \times 16.5 \times 0.75$ mm^3. This strip is placed on the large bottom mold. By pressing the small molds one by one on the strip, a square wave shape is formed in the strip. The mold is thereafter placed in a preheated oven at 80 °C (for 1 h). Because of the faster reaction dynamics of the DA reaction at higher temperatures, stresses induced by the pressing the strip in the mold are relaxed, and the strip takes on the square wave shape.
D. A thin r4/6-strip of $105 \times 17 \times 0.75$ mm^3 is placed on a Teflon plate and the mold is placed on top, such that the square wave strip makes contact with the sheet. This sheet acts as the vertical side membrane of the actuator. The two r4/6-parts are connected through a merging procedure at 80 °C (1 h). The procedure is repeated for a second vertical side membrane on the other side.
E. The r4/6-part is de-molded from the large bottom mold.
F. The small molds can be removed.
G. A strip of 100x16.5x1.5 mm^3 is cut from a synthesized r1-sheet. The air chambers are sealed from the surroundings by placing the r4/6-part (red) on top of this r1 strip (purple) and heating it to 80 °C for 1 h.
H. A hole is made at the back of the actuator in which a Tygon R3603 tube (outer diameter 6.5 mm, inner diameter 5.5 mm) is inserted. The connection between the membrane and this tube is made airtight through another local heating procedure using the hot soldering tool (120 °C).
I. The entire actuator is placed for at last one hour at 80 °C, to form strong interfacial bonds between the different sheets. After this last heating stage, the actuator is left untouched for 24 h at 25 °C. The actuator is airtight and ready to use.

3.4. Validation of the Mechanical Properties

Five multi-material BSPAs were constructed, to be combined in a soft gripper and in a soft hand. To characterize the bending trajectory of the multi-material pneumatic fingers, they were connected to a controlled pressure setup in which five pressures can be controlled individually (details in [27]). By gradually increasing the overpressure of the air chambers and measuring the position using a digital camera (Figure 10), the deformation trajectory was derived, as well, as the relation between the bending angle and the overpressure (Figure 11). This is done for the five multi-material BSPAs in two positions: the actuator is placed vertically with its tip upwards and with its tip downwards (Figure 10A,B). From Figure 11A,C it can be seen that in both positions, tip upwards and tip downwards, the same trajectory is followed by the 5 actuators. A similar trajectory characteristic is one of the requirements when the actuators are used in a gripper, where they are actuated simultaneously to pick objects. In Figure 12, the characteristics for the two configurations, tip upwards and downwards, are compared. The same trajectory is followed in both cases, which indicates that the trajectory of the tip is also independent from the direction of gravity relative to it.

Comparing the bending characteristic of the actuators (Figure 11B,D) it can be observed that they are slightly different. The reason is that the FCB-manufacturing process is preformed manually leading to slight differences in the prototypes. Consequently, all actuator were calibrated prior to use in an application. The relation between the bending angle and the overpressure of the air-chamber, is affected by the direction of the gravitational field, as observed in Figure 12. This highlights the importance of adding force feedback or gravity compensation to the controller of these soft actuators. The model-free feedforward controller used in this work is insufficient, because the response characteristic of the actuators changes when rotating the gripper. Feedback control requires the integration of (a) sensor(s)

in actuator. To not lose the desired flexible characteristic of the soft actuator, the integrated sensor will have to be soft as well. In general, in many soft robots, feedback control is required, hence recently soft sensors are embedded in soft robotic components [5,32–34].

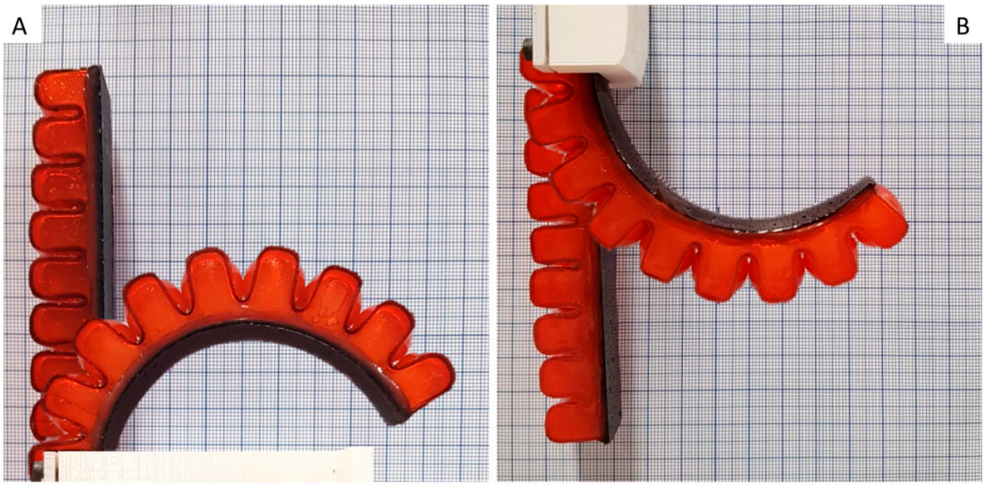

Figure 10. Measuring the deformation trajectory and the relation between bending angle and overpressure for the multi-material BSPA, using a digital camera. The characteristics are derived for two cases: when the BSPA is mounted vertically with the tip facing up (**A**) and down (**B**).

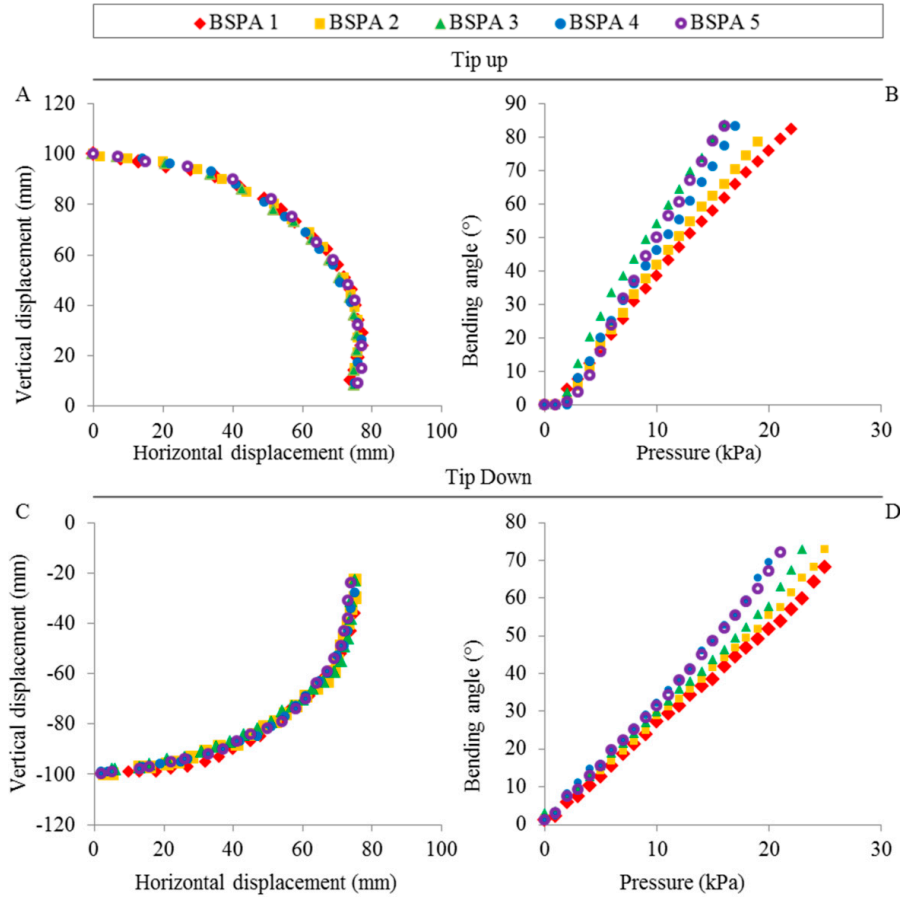

Figure 11. Characterization of the multi-material BSPAs. The deformation trajectory (**A**,**C**) and the bending angle (**B**,**D**) were measured as a function of the overpressure for five actuators, both when the actuators are mounted with the tip facing up and with the tip facing down.

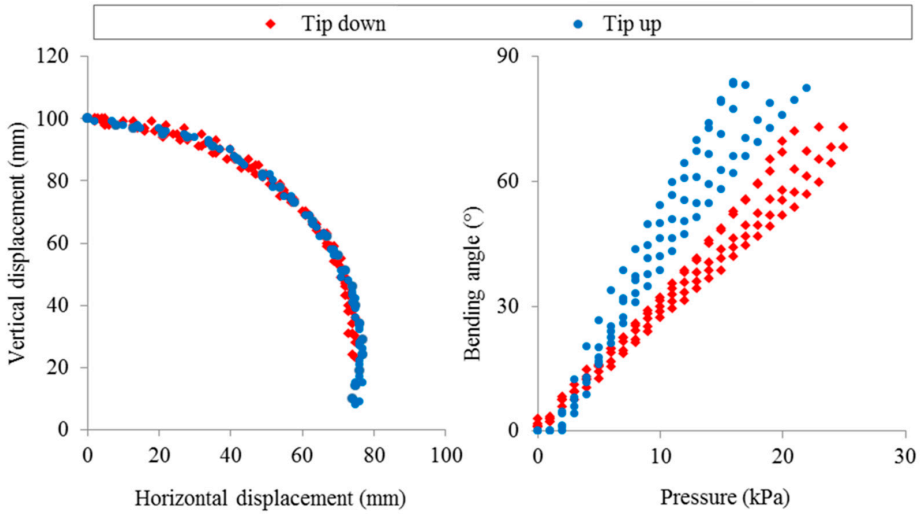

Figure 12. Measuring the deformation trajectory and the relation between bending angle and overpressure for the multi-material BSPA using a digital camera. The characteristics are derived for two cases: when the BSPA is mounted vertically with the tip facing up (**A**) and down (**B**).

To illustrate that these mechanical properties are sufficient for soft robotic applications, four BSPAs were placed in a 3D printed PLA part to form a soft pneumatic gripper (Figure 13). Pressures inside the air chambers of the actuators can be controlled individually using pressure control system [27]. The gripper can pick and place various objects with different shapes (Figure 13). Because of the inherent flexibility of the fingers, extensive control is not needed to grasp objects. The r4/6 (red) DA network used is very flexible, and therefore high deformations can be reached for pressures as low as 20 kPa (Figure 11). However, due to this high flexibility only relatively light objects (egg = 60 g) can be picked up. The maximum weight depends on the shape off the object and the roughness of its surface. It can be increased by making the fingers less flexible by using a stiffer DA network with different network design parameters, or by making the membrane of the BSPA thicker. In general, the healability of more flexible DA networks is higher. Therefore, when evolving towards industrial self-healing soft grippers in the future, it is recommended to decrease the flexibility of the finger by increasing the thickness of the membrane rather than by using less flexible DA networks. When placing five of the healable BSPAs in a 3D printed PLA palm, a soft pneumatic hand is formed (Figure 14). Using the pressure control system all fingers can be actuated individually, which allows performing very simplistic gestures, which can be exploited in social robotics.

Figure 13. Four BSPAs can work together in a soft gripper that allows picking and placing different objects through pressurizing and depressurizing the air chambers.

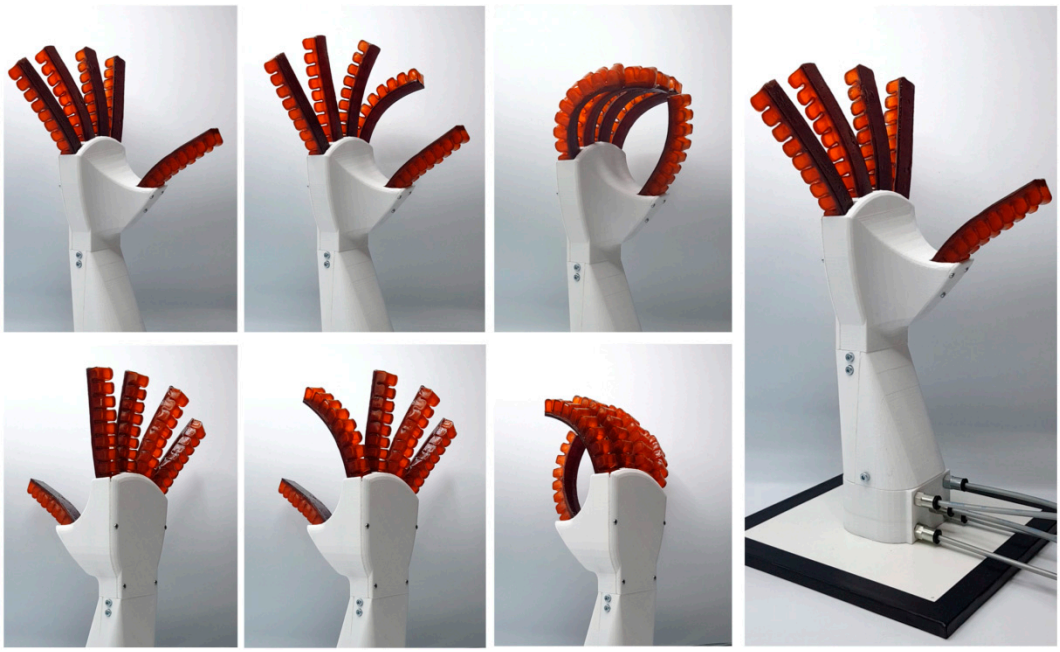

Figure 14. The five BSPAs can be placed on a printed palm to form a soft hand. The fingers can be actuated independently. Because of the flexibility of the hand that ensures safety, it can be used on social robots in the future.

3.5. Validation of the Healing Properties

The healing ability of the BSPA is tested through multiple damage-healing cycles in which macroscopic damages created in the membranes using scalpel blades and needles are healed (Figure 15: Damages D1-D4). Damages were made in both DA networks, in the top r4/6-part (red) and in the bottom r1-layer (purple). The resulting cuts (length > 10 mm) and holes (diameter > 2 mm), which went all the way through the membrane, could all be healed using an external healing procedure in an oven with maximum temperature of T_{max} = 90 °C and t_{iso} = 40 min (Figure 4). After each damage-healing, the pneumatic actuator is again completely airtight. To push the healing ability to its limits, one of the BSPAs was cut completely in half (Figure 15: D5). Both the r4/6 and r1 sections are completely cut through. The halves were manually pressed back together, and the actuator was placed in an oven and healed. After healing, the two parts were merged together, and the actuator was again airtight. This proves that very drastic damages can be healed.

To test the recovery of the mechanical performance of the actuator, its bending characteristic was remeasured after each damage-healing cycle and compared to the initial characteristic prior to damage (Figure 16). After every cycle, the full bending range up to 90° could be covered without the formation of a leak. After each damage-healing cycle a very similar bending characteristic is measured, which illustrates excellent recovery after healing. As they are as good as new after complete healing, the actuators can regain their tasks, with initial performance. After being damaged and healed five times in a row, the BSPA was pushed to its limits by increasing gradually the pressure. At 39 kPa the actuator failed at the location indicated in Figure 15 with an asterisk. This failure is not at the interface between the two different DA networks nor at the location of a healed damage, which demonstrates that a very strong interfacial bond was created between the two materials during manufacturing and no weak spots are created after healing.

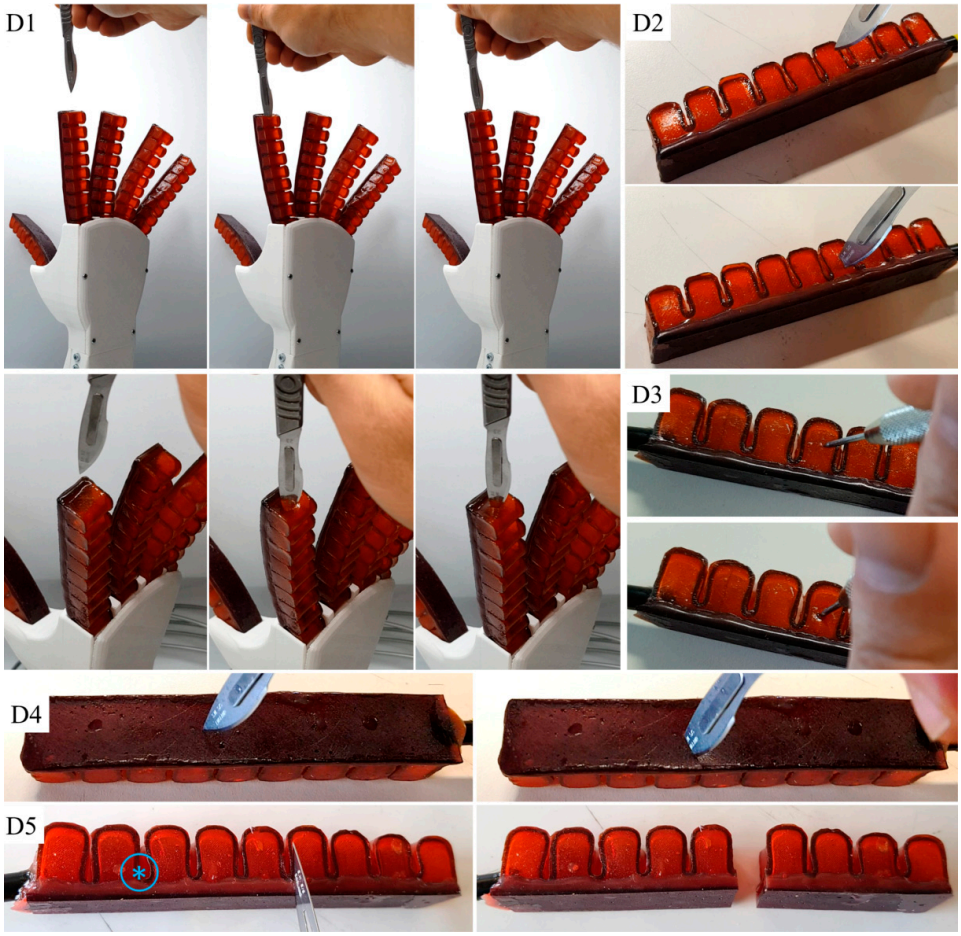

Figure 15. The healing ability of the improved BSPA is tested through the healing of macroscopic damages induced by sharp objects, such as a scalpel blade (Damage D1, D2, D4 and D5) and a needle (D3). Relatively large cuts of > 10 mm can be completely healed using mild heating (90 °C). After healing, the actuators are again completely airtight and all that remains is a very shallow scar due to misalignment.

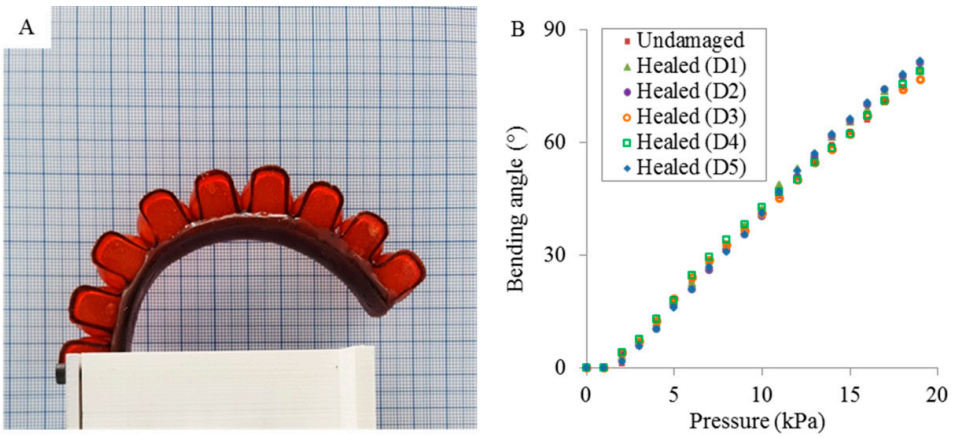

Figure 16. (**A**) After being cut completely in half, BSPA 2 was healed using a healing procedure that involved heating the finger to 90 °C. After healing, the BSPA was again in one piece and the damage was completely recovered. The actuator was again airtight and could be actuated by compressed air. (**B**) The healed BSPA 2 shows a very similar bending characteristic before damage and after every damage-healing cycle.

In fact, the size of the damage that is still healable is mainly limited by the ability to make contact between the fracture surfaces. Upon healing material cannot be grown or created, and therefore large holes, shears or cuts where the cut/fracture surfaces do not touch, cannot be healed. On the other hand, very large damage where contact can again be made can be healed, as illustrated by the actuator that was cut in half. Of course, the healing was performed in a clean lab environment. When going towards industrial or commercial applications of these self-healing soft robotic components it is important to investigate the influence of dust and dirt particles that can contaminate the fracture surface. Because the DA networks do not dissolve in water, a cleaning process that involves spraying water to clean the fracture surfaces might be interesting to investigate. Dust and dirt can also be removed from the fracture surfaces using a compressed air gun. The latter cleaning system might be more convenient to implement, since in soft pneumatic robotic systems a compressed air source is already available.

4. Discussion

The connections between flexible materials in soft robots are generally weak, because they rely fully on physical adhesion. After several actuating cycles or when overloaded, it is at these interfaces, where stress concentrations build up, that the components fail. Diels–Alder (DA) elastomers, which can be synthesized for selected mechanical properties, can provide an answer to this problem. As all DA networks contain the same (reversible) DA crosslinks, strong covalent bonds can be formed across the contact interface between two different DA materials, using a mild heating procedure (85–90 °C). It was experimentally proven through tensile testing that covalent bonds provide high interfacial strength, such that the interface between two DA materials is stronger than the weakest of the two materials and no longer the weakest spot, as is often the case in soft robotics where other bonding techniques are used, relying on physical interactions.

This merging principle between two different DA materials is exploited in the manufacturing of a multi-material BSPA, which relied on a novel shaping technique noted folding and covalently binding. All parts of this DA-based bending actuator are chemically bound, ensuring robust connections. The presented merging technique will allow constructing future robust soft robots, in which multiple materials can be combined to generate new, more complex deformation modes and enhance actuator performance, while increasing the lifetime due to the high interfacial strength of the merged regions.

The applicability of the multi-material actuator types is illustrated by placing four of them together to form a soft gripper. This was designed to handle soft objects with great care. Objects with varying shape and size could be grasped and handled. Five of the multi-material soft pneumatic actuators were used to form a soft hand that illustrates the suitability of these DA networks for social robotic applications. As they are entirely made out of Diels–Alder networks, the BSPAs are able to heal from large macroscopic damages, such as cuts and perforations, using mild heating with maximum temperatures of 90 °C and a total duration of 24 h. Even severe damage, such as cutting the actuator into two pieces, can be healed completely, while recovering the initial actuator performance. This healing ability can potentially increase the lifetime of multi-material soft robotics components further, decreasing the required maintenance and the ecological footprint. In addition, DA polymers are completely recyclable as proven in [27].

The capability of combining more than one flexible material in a single soft component highly increases the design freedom for future soft robotics. In the near future, new soft robotic components can be manufactured, in which more than two DA network types can be combined to generate robust parts with interesting deformation modes and an intrinsic healing ability.

Author Contributions: S.T. performed the synthesis, characterization of the DA material and the actuators and validated the healing ability. E.R. assisted in the characterization of the DA materials. J.B. performed fundamental research on the DA polymers required to design and synthesize these polymers. S.T. prepared the manuscript. G.V.A. and B.V. supervised the scientific methodology and did the funding acquisition. All authors read and agreed to the published version of the manuscript.

Funding: This research is funded by the FWO (Fonds Wetenschappelijk Onderzoek) in personal grants of Terryn (1100416N), Brancart (12W4719N) and Roels (1S84120N) and by the EU FET Project SHERO (828818)

Conflicts of Interest: The authors declare no conflict of interest.

References

1. Laschi, C.; Mazzolai, B.; Cianchetti, M. Soft robotics: Technologies and systems pushing the boundaries of robot abilities. *Sci. Robot.* **2016**, *1*, eaah3690. [CrossRef]
2. Rus, D.; Tolley, M.T. Design, fabrication and control of soft robots. *Nature* **2015**, *521*, 467–475. [CrossRef]
3. Marchese, A.D.; Katzschmann, R.K.; Rus, D. A Recipe for Soft Fluidic Elastomer Robots. *Soft Robot.* **2015**, *2*, 7–25. [CrossRef] [PubMed]
4. Walker; Zidek; Harbel; Yoon; Strickland; Kumar; Shin Soft Robotics: A Review of Recent Developments of Pneumatic Soft Actuators. *Actuators* **2020**, *9*, 3. [CrossRef]
5. Polygerinos, P.; Correll, N.; Morin, S.A.; Mosadegh, B.; Onal, C.; Petersen, K.H.; Cianchetti, M.; Tolley, M.T.; Shepherd, R.F. Soft Robotics: Review of Fluid-Driven Intrinsically Soft Devices; Manufacturing, Sensing, Control, and Applications in Human-Robot Interaction. *Adv. Eng. Mater.* **2017**, *19*, 1700016. [CrossRef]
6. Gorissen, B.; Reynaerts, D.; Konishi, S.; Yoshida, K.; Kim, J.; Volder, M. De Elastic Inflatable Actuators for Soft Robotic Applications. *Adv. Mater.* **2017**, *29*, 1604977. [CrossRef] [PubMed]
7. Van Damme, M.; Beyl, P.; VanderBorght, B.; Versluys, R.; Van Ham, R.; Vanderniepen, I.; Daerden, F.; Lefeber, D. The Safety of a Robot Actuated by Pneumatic Muscles—A Case Study. *Int. J. Soc. Robot.* **2010**, *2*, 289–303. [CrossRef]
8. Choi, T.-Y.; Choi, B.-S.; Seo, K.-H. Position and Compliance Control of a Pneumatic Muscle Actuated Manipulator for Enhanced Safety. *IEEE Trans. Control. Syst. Technol.* **2010**, *19*, 832–842. [CrossRef]
9. VanderBorght, B.; Verrelst, B.; Van Ham, R.; Van Damme, M.; Beyl, P.; Lefeber, D. Development of a compliance controller to reduce energy consumption for bipedal robots. *Auton. Robot.* **2008**, *24*, 419–434. [CrossRef]
10. Ranzani, T.; Gerboni, G.; Cianchetti, M.; Menciassi, A. A bioinspired soft manipulator for minimally invasive surgery. *Bioinspiration Biomim.* **2015**, *10*, 35008. [CrossRef]
11. Polygerinos, P.; Wang, Z.; Galloway, K.C.; Wood, R.J.; Gafford, J.B. Soft robotic glove for combined assistance and at-home rehabilitation. *Robot. Auton. Syst.* **2015**, *73*, 135–143. [CrossRef]
12. Shintake, J.; Cacucciolo, V.; Floreano, D.; Shea, H. Soft Robotic Grippers. *Adv. Mater.* **2018**, *30*, 1707035. [CrossRef] [PubMed]
13. Hughes, J.; Culha, U.; Giardina, F.; Guenther, F.; Rosendo, A.; Iida, F. Soft Manipulators and Grippers: A Review. *Front. Robot. AI* **2016**, *3*, 20. [CrossRef]
14. Available online: http://www.softroboticsinc.com/ (accessed on 25 April 2020).
15. Kim, S.; Laschi, C.; Trimmer, B. Soft robotics: A bioinspired evolution in robotics. *Trends Biotechnol.* **2013**, *31*, 287–294. [CrossRef] [PubMed]
16. Scharff, R.B.; Wu, J.; Geraedts, J.M.; Wang, C.C. Reducing Out-of-Plane Deformation of Soft Robotic Actuators for Stable Grasping. In Proceedings of the 2019 2nd IEEE International Conference on Soft Robotics (RoboSoft), Seoul, Korea, 14–18 April 2019; pp. 265–270.
17. Scharff, R.B.; Wu, J.; Geraedts, J.M.; Wang, C.C. A soft exoskeleton for hand assistive and rehabilitation application using pneumatic actuators with variable stiffness. In Proceedings of the 2015 IEEE International Conference on Robotics and Automation (ICRA), Seattle, WA, USA, 26–30 May 2015; pp. 4967–4972.
18. Manti, M.; Hassan, T.; Passetti, G.; D'Elia, N.; Laschi, C.; Cianchetti, M. A Bioinspired Soft Robotic Gripper for Adaptable and Effective Grasping. *Soft Robot.* **2015**, *2*, 107–116. [CrossRef]
19. Schaffner, M.; Faber, J.A.; Pianegonda, L.; Rühs, P.A.; Coulter, F.; Studart, A.R. 3D printing of robotic soft actuators with programmable bioinspired architectures. *Nat. Commun.* **2018**, *9*, 878. [CrossRef] [PubMed]
20. Hughes, J.; Maiolino, P.; Iida, F. An anthropomorphic soft skeleton hand exploiting conditional models for piano playing. *Sci. Robot.* **2018**, *3*, eaau3098. [CrossRef]
21. Chubb, K.; Berry, D.; Burke, T. Towards an ontology for soft robots: What is soft? *Bioinspiration Biomim.* **2019**, *14*, 063001. [CrossRef]

22. Beyl, P.; Van Damme, M.; Van Ham, R.; VanderBorght, B.; Lefeber, D. Pleated Pneumatic Artificial Muscle-Based Actuator System as a Torque Source for Compliant Lower Limb Exoskeletons. *IEEE/ASME Trans. Mechatron.* **2014**, *19*, 1046–1056. [CrossRef]
23. Brancart, J.; Verhelle, R.; Mangialetto, J.; Van Assche, G. Coupling the Microscopic Healing Behaviour of Coatings to the Thermoreversible Diels-Alder Network Formation. *Coatings* **2018**, *9*, 13. [CrossRef]
24. Diaz, M.M.; Brancart, J.; Van Assche, G.; Mele, B. Van Room-temperature versus heating-mediated healing of a Diels-Alder crosslinked polymer network. *Polymer* **2018**, *153*, 453–463. [CrossRef]
25. Brancart, J.; Scheltjens, G.; Muselle, T.; Van Mele, B.; Terryn, H.; Van Assche, G. Atomic force microscopy–based study of self-healing coatings based on reversible polymer network systems. *J. Intell. Mater. Syst. Struct.* **2012**, *25*, 40–46. [CrossRef]
26. Scheltjens, G.; Diaz, M.M.; Brancart, J.; Van Assche, G.; Van Mele, B. Thermal evaluation of a self-healing polymer network coating based on reversible covalent bonding. Reactive and Functional. *Polymers* **2013**, *73*, 413–420.
27. Terryn, S.; Brancart, J.; Lefeber, D.; Van Assche, G.; VanderBorght, B. Self-healing soft pneumatic robots. *Sci. Robot.* **2017**, *2*, eaan4268. [CrossRef]
28. Roels, E.; Terryn, S.; Brancart, J.; Van Assche, G.; VanderBorght, B. A Multi-Material Self-Healing Soft Gripper. In Proceedings of the 2019 2nd IEEE International Conference on Soft Robotics (RoboSoft), Seoul, Korea, 14–18 April 2019; pp. 316–321.
29. Terryn, S.; Brancart, J.; Lefeber, D.; Van Assche, G.; VanderBorght, B. A Pneumatic Artificial Muscle Manufactured Out of Self-Healing Polymers That Can Repair Macroscopic Damages. *IEEE Robot. Autom. Lett.* **2017**, *3*, 16–21. [CrossRef]
30. Mosadegh, B.; Polygerinos, P.; Keplinger, C.; Wennstedt, S.; Shepherd, R.F.; Gupta, U.; Shim, J.; Bertoldi, K.; Gafford, J.B.; Whitesides, G.M. Pneumatic Networks for Soft Robotics that Actuate Rapidly. *Adv. Funct. Mater.* **2014**, *24*, 2163–2170. [CrossRef]
31. Martinez, R.; Fish, C.; Chen, X.; Whitesides, G.M. Elastomeric Origami: Programmable Paper-Elastomer Composites as Pneumatic Actuators. *Adv. Funct. Mater.* **2012**, *22*, 1376–1384. [CrossRef]
32. Giffney, T.; Xie, M.; Yong, A.; Wong, A.; Mousset, P.; McDaid, A.; Aw, K.C. Soft Pneumatic Bending Actuator with Integrated Carbon Nanotube Displacement Sensor. *Robotics* **2016**, *5*, 7. [CrossRef]
33. Morrow, J.; Shin, H.-S.; Phillips-Grafflin, C.; Jang, S.-H.; Torrey, J.; Larkins, R.; Dang, S.; Park, Y.-L.; Berenson, D. Improving Soft Pneumatic Actuator fingers through integration of soft sensors, position and force control, and rigid fingernails. In Proceedings of the 2016 IEEE International Conference on Robotics and Automation (ICRA), Stockholm, Sweden, 16–21 May 2016; pp. 5024–5031.
34. Thuruthel, T.G.; Shih, B.; Laschi, C.; Tolley, M.T. Soft robot perception using embedded soft sensors and recurrent neural networks. *Sci. Robot.* **2019**, *4*, eaav1488. [CrossRef]